Mechanism of HO_x Formation in the Gas-Phase Ozone-Alkene Reaction. 2. Prompt versus Thermal Dissociation of Carbonyl Oxides to Form OH

Jesse H. Kroll,* Shailesh R. Sahay, and James G. Anderson

Department of Chemistry and Chemical Biology, Harvard University, Cambridge, Massachusetts 02138

Kenneth L. Demerjian

Department of Earth and Atmospheric Sciences, and Atmospheric Sciences Research Center, SUNY−Albany, New York 12203

Neil M. Donahue‡

Departments of Chemistry and Chemical Engineering, Carnegie Mellon University, Pittsburgh, Pennsylvania 15213

Received: November 9, 2000

In a companion paper (Kroll, J. H.; Clarke, J. S.; Donahue, N. M.; Anderson, J. G.; Demerjian, K. L. *J. Phys. Chem. A* **2001**, *105*, 1554) we present direct measurements of hydroxyl radical (OH) yields for the gas-phase reaction of ozone with a number of symmetric alkenes. Yields are strongly pressure-dependent, contrary to the results of prior scavenger studies. Here we present a statistical-dynamical model of OH production from the reaction, utilizing RRKM/master equation calculations to determine the fate of the carbonyl oxide intermediate. This model agrees with our experimental results, in that both theory and observations indicate strongly pressure-dependent OH yields. Our calculations also suggest that ethene ozonolysis produces OH via a different channel than the substituted alkenes, though the identity of this channel is not clear. This channel may play a role in the ozonolysis of monosubstituted alkenes as well. Our time-dependent master equation calculations show that the discrepancy between OH yields measured in our direct study and those measured in prior scavenger studies may arise from differing experimental time scales; on short time scales, OH is formed only from the vibrationally excited carbonyl oxide intermediate, whereas on longer time scales OH formation from thermal dissociation may be significant. To demonstrate this we present time-dependent measurements of OH yields at 10 Torr and 100 Torr; yields begin increasing after hundreds of milliseconds, an effect which is much more pronounced at 100 Torr. These results are entirely consistent with theoretical predictions. In the atmosphere, the thermalized carbonyl oxide may be susceptible to bimolecular reactions which, if fast enough, could prevent dissociation to OH; however there is little experimental evidence that any such reactions are important. Thus we conclude that both mechanisms of OH formation (dissociation of vibrationally excited carbonyl oxide and dissociation of thermalized carbonyl oxide) are significant in the troposphere.

Introduction

A major obstacle in elucidating complex gas-phase reaction mechanisms is determining the role of highly excited (chemically activated) intermediates. Multiple reaction pathways may be available, leading to any number of possible reaction products; such products in turn may be extremely reactive as well. Collisional stabilization by bath gas molecules may compete with unimolecular reaction, leading to pressure-dependent product yields. Further, prompt reaction or collisional stabilization usually cause such intermediates to have extremely short lifetimes, making detection extremely difficult.

The uncertainty in the mechanism of hydroxyl (OH) radical formation from the gas-phase ozone-alkene reaction highlights such difficulties. Indirect[2−7] and direct[1,8,9] measurements have established that OH is indeed formed in this reaction, and modeling calculations[10,11] indicate that that this may be an important source of HO_x in the troposphere. Still, details of the reaction mechanism remain highly uncertain. The reaction is believed to proceed via a number of short-lived, highly excited intermediates, most notably the carbonyl oxide (see Mechanism section, below); however, few such intermediates have been detected in the gas phase. Furthermore, most experiments to determine product yields are carried out over long time scales, often several minutes to hours, which is a poor match to the time scales of these intermediates. Due to the high reactivity of the reaction intermediates and products, it is difficult to determine which species measured in these experiments are prompt products and which are byproducts of unwanted secondary reactions.

As a stark example of these difficulties, our own measurements of the pressure dependence of OH yields from ozone−alkene reactions appear to disagree markedly from indirect measurements of the same systems. We have directly measured the pressure dependence of prompt OH production[1] on a 10 ms

* Corresponding author. E-mail: kroll@fas.harvard.edu.
‡ E-mail: nmd@andrew.cmu.edu.

10.1021/jp004136v CCC: $20.00
Published on Web 04/12/2001

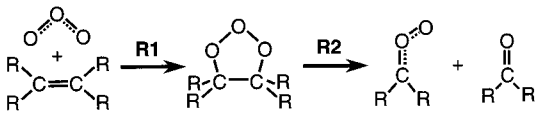

Figure 1. Criegee mechanism of carbonyl oxide formation: ozone−alkene cycloaddition (R1) and subsequent fragmentation (R2) to form the carbonyl oxide.

time scale, finding strongly pressure-dependent yields for all substituted alkenes, with yields at one atmosphere far below unity. Indirect studies, however, have found much higher yields at atmospheric pressure. One such study[12] in fact finds most yields to be largely pressure-independent. The appearance is thus not of a well-understood system, but rather of one with major disagreements among various studies. The objective of this paper is to reconcile many of these disagreements.

Here we present a simple statistical-dynamical model of the ozone−alkene reaction mechanism, utilizing RRKM theory for unimolecular rate constants and the time-dependent master equation to describe the effects of collisions with the bath gas. The goal of this model is 3-fold. First, it allows us to verify whether the accepted reaction mechanism can produce OH in roughly the quantities observed, in either the direct or indirect studies. Second, comparison of theory and experiment may allow us to better understand what factors control prompt OH yield. Finally, it may allow insight into the large discrepancies in the absolute yields and pressure dependences of the two types of studies. The goal of this model is not predictive accuracy but rather qualitative agreement with experiment. Modeling the time-dependent behavior of the system will be a key factor in understanding the differences among the various studies. Our model will offer a specific prediction of the time dependence of OH production, and we shall present experimental confirmation of that prediction.

Mechanism

The initial steps of the gas-phase ozone-alkene reaction mechanism are widely believed to follow the basic Criegee mechanism,[13] as shown in Figure 1 for a symmetric alkene. Ozone adds to the alkene in a concerted [2+3] cycloaddition (reaction R1), forming a primary ozonide. This reaction is highly exothermic (50−60 kcal/mol), and the excited ozonide can quickly dissociate (R2) into a carbonyl oxide (the Criegee intermediate) and a carbonyl species. This step is generally assumed to be concerted but may be stepwise.

In the solution phase the vibrationally excited products are quickly quenched and held closely together by the cage effect, rejoining to form a secondary ozonide. In the gas phase, however, they will separate. The excess vibrational energy is not high enough to lead to any further dissociation of the carbonyl species; however, the carbonyl oxide has sufficient energy to permit further unimolecular reactions.

The carbonyl oxide is generally understood to react by one of two primary channels, isomerization to dioxirane and dissociation to OH.[14,15] The importance of each channel varies depending on the degree of substitution as well as the conformation (syn or anti) of the carbonyl oxide. Figure 2 shows further reactions of the unsubstituted (or monosubstituted anti) carbonyl oxide. Isomerization to dioxirane (reaction R3a) is believed to be followed by a ring cleavage (R3b) to form a singlet biradical dioxyalkane. This in turn is believed to isomerize (R3c) to form a vibrationally excited ("hot") organic acid, which may dissociate (R3d) to one of many sets of products, including OH, H, and R radicals. Alternately, the

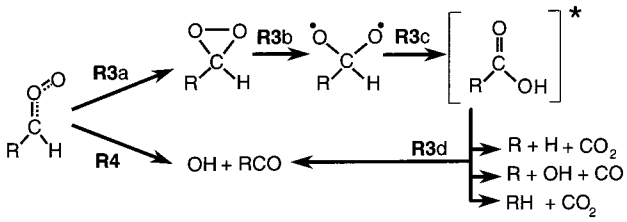

Figure 2. Unimolecular reaction channels available to the unsubstituted (or monosubstituted anti) carbonyl oxide: isomerization to dioxirane (R3a), which eventually leads (R3b−d) to many possible dissociation products, and concerted dissociation (R4) to form OH and RCO.

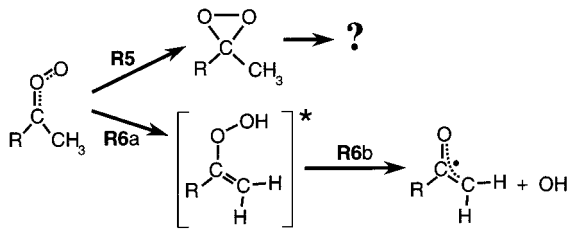

Figure 3. Unimolecular reaction channels available to the substituted carbonyl oxide: isomerization to dioxirane (R5), or isomerization (R6a) to an excited hydroperoxide, which will quickly dissociate (R6b) to OH.

carbonyl oxide may dissociate to OH (reaction R4), in a concerted process[8,16] which occurs via a four-membered transition state.

The reactions of disubstituted (or monosubstituted syn) carbonyl oxides are shown in Figure 3. The dioxirane channel (reaction R5) may occur as in the unsubstituted case, but the identities of further reaction products are highly uncertain. Experiments suggest the "hot ester" analog to the "hot acid" channel (reaction R3) does not occur,[15,17] presumably as it requires an alkyl-transfer rather than a simple H-transfer. A more significant difference between the reactions of substituted and unsubstituted carbonyl oxides is the OH-formation channel: for substituted carbonyl oxides, OH formation is not a concerted process but rather takes place via an excited hydroperoxide intermediate (reaction R6). Formation of this intermediate occurs via a five-membered transition state, and is expected to proceed significantly faster than reaction R4. This is supported by electronic structure and statistical rate calculations by Cremer and co-workers[16,18] and suggests that OH yields from substituted alkenes should be higher than from ethene.

A major point of uncertainty in the above mechanism is the role of collisional activation and deactivation of the reactive intermediates. The carbonyl oxide is the highest in energy (electronically) of the CR_2O_2 intermediates,[8,19] so for a given energy it has the least vibrational excitation and hence the longest lifetime. As a result, it is the most susceptible to stabilization by bath gas molecules. Competition between collisional stabilization and unimolecular reaction would be indicated experimentally by pressure-dependent product yields.

However, on this point there exists conflicting experimental evidence. In general, radical-scavenger studies seem to indicate no pressure dependence; this comes not only from high 1 atm yields measured for a number of alkenes[6] but also from a recent study in which OH yields are measured over a range of pressures.[12] Additionally, if collisional stabilization were to be important, alkene size should have an effect on yield: larger carbonyl oxides have more modes over which excess vibrational energy may be distributed and so will be more susceptible to collisional stabilization. Yet structure−activity relationships (SAR's) for OH yields, based only on the level of substitution

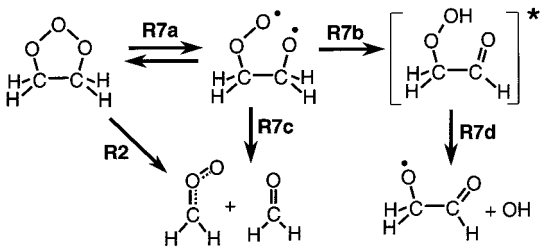

Figure 4. OH formation via nonconcerted decomposition of the primary ozonide.

of a carbonyl oxide (un-, mono- or disubstituted) and not on substituent size or on available vibrational energy, are generally successful in predicting OH yields as measured in scavenger studies.[2,4,6] This lack of a major size-dependent effect suggests no competition between unimolecular reaction and collisional stabilization: either the excited carbonyl oxide undergoes prompt unimolecular reaction with no collisional deactivation, or collisional stabilization dominates and the observed OH is formed entirely from reactions of the thermalized carbonyl oxide.

On the other hand, our direct measurements[1] indicate a substantial pressure dependence for a number of substituted alkenes. In addition, measurements of stabilized carbonyl oxide yields (by addition of SO_2 and detection of H_2SO_4, a product of the $CR_2OO + SO_2$ reaction) indicate a pressure dependence as well.[20] Time-independent master equation results[21] also predict a weak pressure dependence for the OH yield from the ozone−TME reaction.

Another source of uncertainty in the reaction mechanism is the potential importance of additional pathways of prompt OH formation other than the direct formation from carbonyl oxides (reactions R4 and R6). One is the "hot acid" channel, reaction R3. This was first identified in an early study of the ozone-ethene reaction,[22] but is often ignored in the recent literature,[16] due to the large enthalpy difference of formic acid and HCO + OH (100 kcal/mol). However, formic acid is formed with far more energy than this, and dissociation to OH proceeds via a loose transition state. The barriers for the $H_2 + CO_2$ and $H_2O + CO$ channels are lower in energy, but are much "tighter" (proceeding by four- and three-membered TS's, respectively) and so are entropically disfavored. Therefore, it is reasonable to assume a fraction of the formic acid will indeed dissociate to OH.

Additionally, it has been suggested[23,24] that nonconcerted decomposition of the ozonide, followed by a 1,4-hydrogen shift, may lead to OH formation via an excited hydroperoxide intermediate (Figure 4). Electronic structure calculations differ on the relative barrier heights of the individual steps and thus on the importance of this additional channel.[12,25]

The common thread in these mechanisms is the presence of tens to hundreds of kcal/mol of excess vibrational energy in the reaction products. This chemical activation opens multiple possible reaction pathways and sets up a competition between collisional deactivation and further reaction of the vibrationally excited fragments. Because the energies involved are much greater than the typical vibrational energy transfer of a collision, and because the branching is highly energy-dependent, we need to turn to the master equation to gain even qualitative insight into these systems. As we shall see, time dependence is also a crucial component in this case, so we shall next present a concise formulation of the time-dependent master equation.

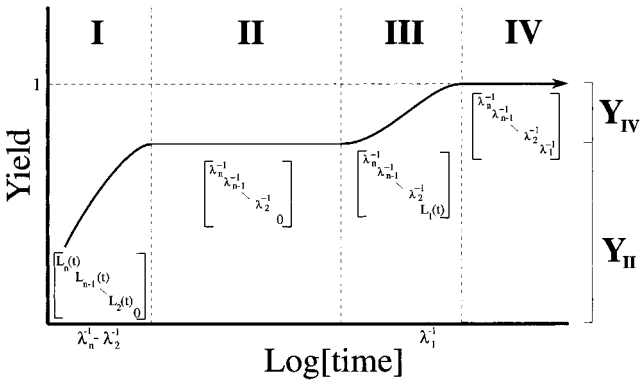

Figure 5. Time-dependent yield for the unimolecular reaction of a chemically activated intermediate. The time-dependent behavior may be divided into four regimes, each with a characteristic expression of the matrix **L** (shown). Regime I (incubation) corresponds to the fast population of the vibrationally excited intermediate. In regime II (pseudo steady state) the chemically activated species has reached steady state and the population of the thermalized intermediate begins to grow. In regime III, thermal reaction becomes important, and in regime IV (steady state), the thermal species has reached true steady state, with product yield of unity and net stabilization zero.

Theoretical

The master equation describing the time-dependent population $\mathbf{N}(t)$ of an intermediate species (in which each element of the vector corresponds to an energy level) is given by[26]

$$\frac{d\mathbf{N}(t)}{dt} = R\mathbf{F} - [\omega(\mathbf{I} - \mathbf{P}) + \sum_i \mathbf{K}_i]\mathbf{N}(t) \equiv R\mathbf{F} - \mathbf{J}\mathbf{N}(t) \quad (1)$$

in which R is the overall rate of intermediate formation, **F** the normalized vibrational population distribution of the nascent intermediate, **P** the normalized energy transfer matrix, **I** the unit matrix, ω the collision frequency, and $\mathbf{K}_i$ a diagonal matrix of unimolecular rate constants for the ith channel. The steady-state solution of eq 1 yields the simple expression $\mathbf{N} = R\mathbf{J}^{-1}\mathbf{F}$. The time-dependent solution, however, has been derived,[27] and may be expressed in terms of the right eigenvector matrix (**U**) and eigenvalues (λ) of **J**:

$$\mathbf{N}(t) = R\mathbf{U}\mathbf{L}\mathbf{U}^{-1}\mathbf{F} \quad (2)$$

where **L** is a diagonal matrix with diagonal elements i equal to $(1 - e^{-\lambda_i t})/\lambda_i$. A derivation of this formulation is provided in Appendix A. Given the time-dependent population $\mathbf{N}(t)$, calculating the time-dependent yield $Y(t)$ for the ith channel is straightforward:

$$Y_i(t) = \frac{\sum_E \mathbf{N}(E,t)\mathbf{K}_i(E)}{R} \quad (3)$$

$$= \sum_E [\mathbf{U}\mathbf{L}\mathbf{U}^{-1}\mathbf{F}](E,t)\mathbf{K}_i(E) \quad (4)$$

Therefore, yield does not depend on R, the rate of intermediate formation.

While the full expression for the time-dependent yield is a large polynomial, for real systems it may be simplified significantly. As is characteristic of matrixes describing collisional energy transfer, there is a very large separation between the smallest eigenvalue (λ_1) and the others, which are closely spaced. This separation, usually many orders of magnitude, leads to a characteristic time-dependent yield with four regimes, as shown in Figure 5. Approximate expressions for the matrix **L** are also given.

Regime I is the transient (or "incubation"[28]) period, whose time dependence is governed by all the larger eigenvalues. This corresponds to the formation of the chemically activated intermediate, and occurs extremely quickly, with a time scale on the order of a single collision. Regime II is the period ($(\lambda_n^{-1}$, . . ., $\lambda_2^{-1} \ll t \ll \lambda_1^{-1}$) in which the excited intermediate has reached steady state with respect to unimolecular reaction and collisional stabilization. This is called the "pseudo steady state"[29] or "intermediate steady state"[28] and is characterized by an essentially time-independent yield. This is generally the time scale on which chemical activation experiments are performed, and may be modeled with a deactivating form of the steady-state master equation, in which a reactant sink slightly below reaction threshold is imposed. The "semistrong collision" approach[30] has also been used to model the behavior of chemical activation systems successfully.[31]

Once the time scale approaches λ_1^{-1}, corresponding to the time scale of thermal reaction, the yield begins increasing again (regime III); this corresponds to the unimolecular reaction of the thermalized species. Finally, in regime IV ($t \gg \lambda_1^{-1}$), the intermediate has reached true steady state (the "long steady state"[28]) in which the total flux in (rate of formation) equals total flux out (unimolecular reaction), and net stabilization is zero. It is this regime to which the full steady-state master equation applies.

Note that for regimes II−IV (i.e., the time scales of most experiments), the time dependence of the yield may be expressed simply as

$$Y(t) = Y_{II} + Y_{IV}(1 - e^{-\lambda_i t}) \qquad (5)$$

where Y_{II} is the yield at the pseudo steady state (the "prompt yield") and Y_{IV} the increase in yield once the true steady state has been reached.

The increase in yield in regime III (the second term in eq 5) arises from the large population of thermalized intermediate undergoing unimolecular reaction, but this may not always occur in real systems. If the lifetime of the intermediate with respect to unimolecular reaction (λ_1^{-1}) is long relative to the lifetime versus bimolecular reaction (or relative to the time scale of the experiment), the long steady state (regime IV) is never reached. This is usually the case in chemical activation experiments: either the thermalized product is extremely stable and will not undergo unimolecular reaction on a reasonable time scale, or it is reactive and will be rapidly scavenged by oxygen, effectively removing it from the system. Thus it is common to ignore the true steady state, assuming that only the pseudo steady state is relevant on experimental time scales.[28,29]

For species with low barriers to unimolecular reaction, however, this assumption is not always valid (see, for example, ref 32 and references within). In the present case, the carbonyl oxide has thermally accessible unimolecular reaction channels (with barriers below 20 kcal/mol), and is known to be unreactive with oxygen. Therefore, the lifetime of the stabilized carbonyl oxide may be long enough such that thermal dissociation to OH (in regimes III and IV) may occur. This may or may not be significant under atmospheric conditions, depending on the thermal lifetime of the intermedate and the rates of any competing bimolecular reactions. On the other hand, any OH formed in regime II (from the vibrationally excited carbonyl oxide) will certainly be significant under all conditions, as it is formed on a time scale far faster than that of any secondary bimolecular reaction. Thus we focus first on the OH formed by the vibrationally excited carbonyl oxide (regime II), which (assuming $\lambda_1^{-1} > 10$ ms) is the regime in which our prompt measurements[1] are made. We will discuss the time-dependent behavior of the system in a later section.

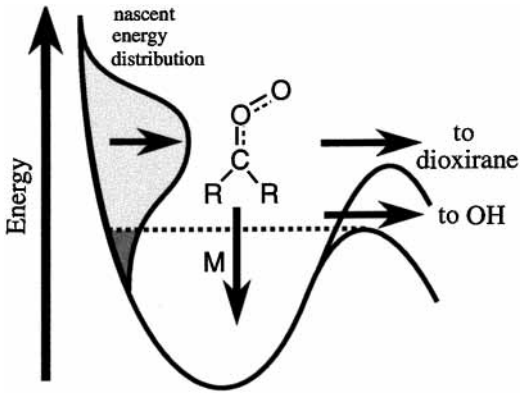

Figure 6. The system modeled in our master equation calculations. The carbonyl oxide is formed with some nascent energy distribution from the dissociating ozonide; some fraction is below reaction threshold, corresponding to carbonyl oxide formed vibrationally "cold". The "hot" carbonyl oxide may either be collisionally stabilized or may react, to form OH or dioxirane. For unsubstituted carbonyl oxides, the relative ordering of the transition states are opposite that shown.

Olzmann et al.[21] have performed steady-state master equation calculations (in regime II only) of the ozonolysis of two alkenes, ethene and 2,3-dimethyl-2-butene (tetramethylethyene, or TME). Here we perform calculations for all six symmetric alkenes covered in our experimental study: ethene, TME, 3,4-dimethyl-3-hexene, *trans*-2-butene, *trans*-3-hexene, and *trans*-4-octene. Modeling all the alkenes in this series allows us not only to assess whether our measured pressure-dependent yields are reasonable, but also to determine what factors control OH yield.

We apply the master equation to the carbonyl oxide only. Substituted carbonyl oxides do not dissociate to OH directly but rather via a hydroperoxide intermediate (reaction R6). However, this intermediate is much more stable than the carbonyl oxide and dissociates to OH via a loose transition state, so the yield of hydroperoxide dissociation to OH is expected to be near unity and pressure-independent; this has been validated by SACM calculations in ref 21. This means isomerization to hydroperoxide is the rate-limiting step in the formation of OH from the carbonyl oxide, and we may safely ignore the hydroperoxide intermediate. Similarly, we also do not model the behavior of the ozonide. We have performed full master equation calculations on the ozonide from ozone + ethene, finding that collisional stabilization of the ozonide is too slow to compete with fragmentation. This conclusion was also reached by Olzmann et al. for ethene as well as TME.[21] The level of vibrational excitation is so high that the ozonides formed from larger alkenes in this study (such as *trans*-4-octene and 3,4-dimethyl-3-hexene) are also not expected to be collisionally stabilized; indeed, there exists no experimental evidence of gas-phase primary ozonide thermalization. We assume the ozonide only decomposes, forming carbonyl oxide (reactions R2 and R7c), and does not isomerize (reaction R7d); we will address this point in a later section.

The modeled system is shown in Figure 6. A fraction of the nascent carbonyl oxde is formed "cold", without enough internal energy to react. The remainder will react to form OH or dioxirane, or be collisionally stabilized. To solve the master equation, three parameters must be known: microcanonical rate constants, collisional energy transfer probabilities, and the energy distribution of the nascent species. Methods of obtaining

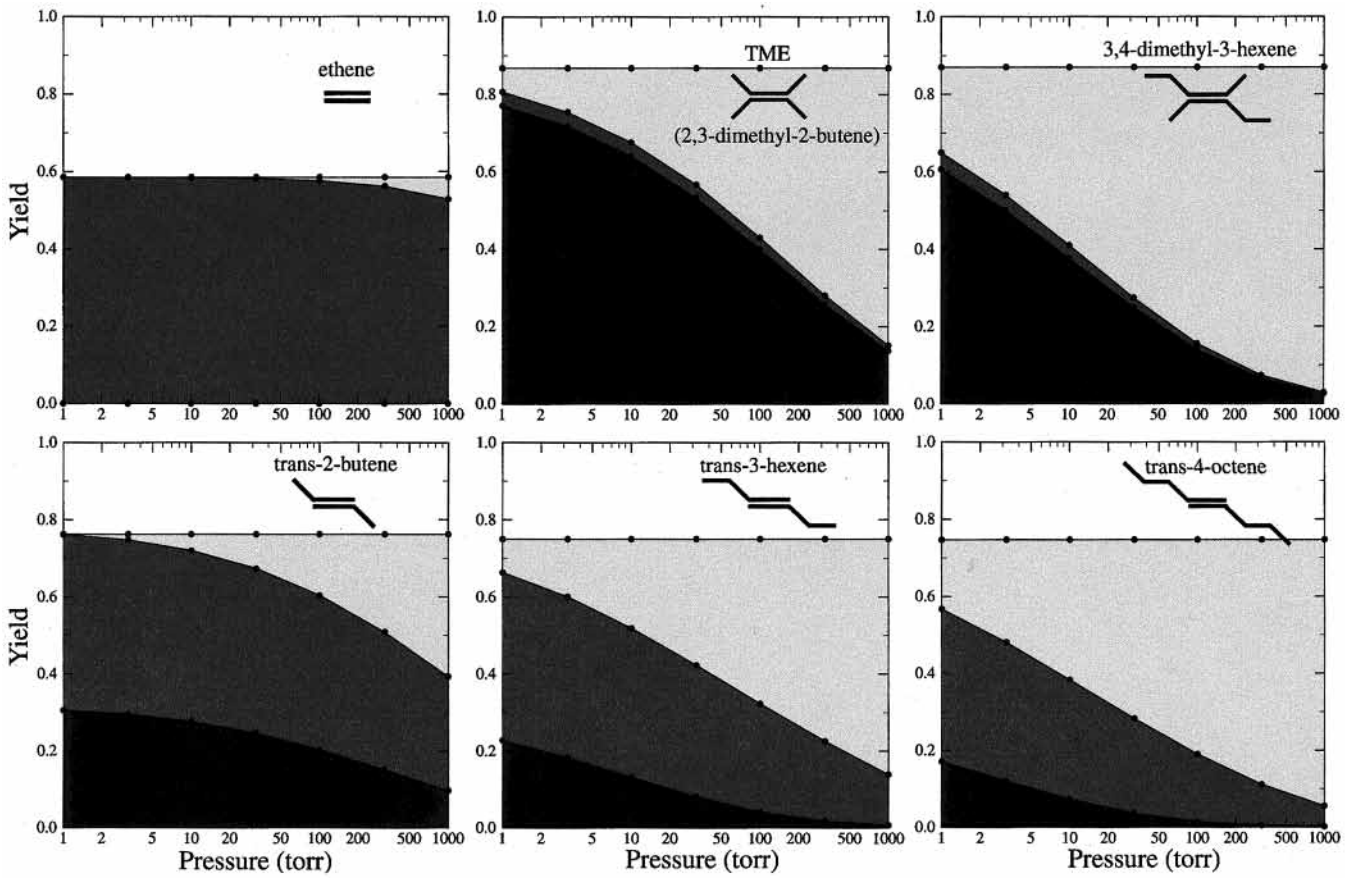

Figure 7. Calculated prompt yields for the ozonolysis of the six alkenes covered in this study, as a function of pressure (in Torr). Shading indicates product: OH (black), dioxirane (dark gray), collisionally stabilized carbonyl oxide (light gray) or carbonyl oxide formed vibrationally "cold" (white). Black dots indicate pressures at which calculations were performed.

values for these parameters are described in detail in Appendix B.

Results

Master equation results for regime II, the psuedo steady-state case, are shown in Figure 7 for the six symmetric alkenes. We divide the reaction into four distinct pathways: prompt generation of OH, prompt generation of dioxirane, collisional stabilization of carbonyl oxide, and formation of "cold" carbonyl oxide. Yields are calculated at 7 pressures (1, 3.2, 10, 32, 100, 320, and 1000 Torr) for each alkene. In all cases the average energy lost per deactivating collision ($\langle \Delta E \rangle_d$) is set to 500 cm^{-1}. Sums and densities of states were calculated at 1 cm^{-1} intervals; for computational efficiency, these were binned into master equation grain sizes of 50 cm^{-1}. We found that yields obtained using finer energy-graining differ by no more than a few percent. There are a number of potential sources of error in these calculations, including our use of a simple model for energy transfer probability (which employs an uncertain $\langle \Delta E \rangle_d$), inherent errors in the electronic structure calculations, uncertainty in the energy distribution of the nascent carbonyl oxide, and errors introduced by neglecting tunneling effects (which may be particularly important for the OH-formation channel, which is largely an H-transfer). As a result, we have tested the sensitivity of our results to many of these potential sources of error. Sample results from these calculations are provided in Appendix C; results indicate that while changing such parameters can make a significant difference in the calculated yields, the differences are not substantial enough to affect our fundamental conclusions.

In the case of ethene, we predict that almost no OH (<1% yield) will be formed from direct dissociation of the carbonyl oxide, as this is not the lowest-barrier channel. Instead, all of the carbonyl oxide which is formed vibrationally "hot" (i.e., with enough energy to react) will isomerize to dioxirane. The rate of isomerization is faster than the rate of collisional deactivation, so only a very weak pressure dependence of the dioxirane yield is predicted. Still, much of the carbonyl oxide is formed vibrationally "cold" and cannot undergo prompt unimolecular dissociation.

For the disubstituted carbonyl oxide (from TME), the barrier to OH formation is significantly lower, so a smaller fraction of the carbonyl oxide is formed vibrationally "cold". Instead, at low pressures at least, formation of OH dominates, with little dioxirane (<5%) formed. At higher pressures, the rate of stabilization is competitive with that of OH formation, so highly pressure-dependent OH yields are predicted.

Our ethene and TME results agree qualitatively with those of Olzmann et al.[21] There are, however, significant quantitative differences; for example at 1 atm they predict a TME yield of between 66%-78%, much higher than our predictions. However, in Appendix C we show that such differences may arise from relatively small changes in parameters. Thus we do not concern ourselves with these discrepancies, which could arise from any number of factors: differences in electronic structure results, energy transfer models (exponential-down vs stepladder), collision frequency ω, etc.

The results for 3,4-dimethyl-3-hexene are qualitatively similar to those of TME, as OH yield is also expected to be strongly pressure-dependent. However, the pressure dependence is stronger than for TME. This is a result of the larger number of vibrational modes in the larger carbonyl oxide over which excess vibrational energy may be distributed. This will lead to a longer

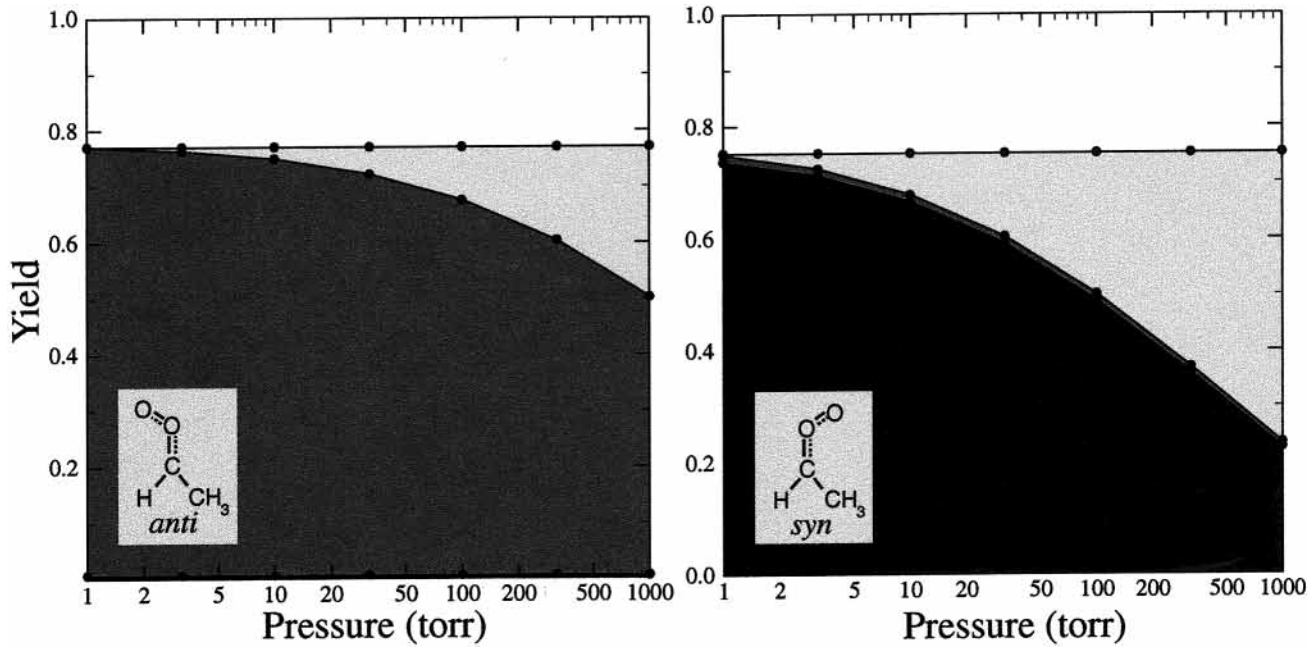

Figure 8. Fate of the anti and syn forms of the monosubstituted carbonyl oxide from *trans*-2-butene. Results are shown as a function of pressure (in Torr). As in Figure 7, shading indicates product: OH (black), dioxirane (dark gray), collisionally stabilized carbonyl oxide (light gray) or carbonyl oxide formed vibrationally "cold" (white). The anti species behaves like an unsubstituted carbonyl oxide, mostly forming dioxirane; the syn species behaves much like the carbonyl oxide from TME, mostly forming OH.

lifetime with respect to reaction and thus greater susceptibility to collisional stabilization. This effect, however, is not particularly strong.

Calculations for the series of disubstituted alkenes (*trans*-2-butene, *trans*-3-hexene, and *trans*-4-octene) require master equation treatments for both the anti and syn conformers, which are believed not to interconvert, due to a large barrier.[33] Yields from the individual conformers from *trans*-2-butene are shown in Figure 8; while the energetics are somewhat different, overall the anti conformer behaves much like an unsubstituted carbonyl oxide (as from ethene), whereas the syn form behaves like a disubstituted carbonyl oxide (as from TME). Overall product yields from *trans*-2-butene are obtained by weighting yields shown in Figure 8 by the relative formation yields of each conformer (see Appendix B). As is to be expected from their barrier heights (Table 2), practically all the dioxirane formed is from the anti species, whereas all the OH formed is from the syn species. Both OH and dioxirane are formed with relatively high yields and are expected to be pressure-dependent. Product yields from *trans*-3-hexene and *trans*-4-octene are found to be more pressure-dependent than for *trans*-2-butene, again due to the larger number of vibrational modes.

Comparison of Theory and Experiment

For all substituted alkenes, our calculations show that OH is indeed expected as a prompt product of the excited carbonyl oxide, with yields that are strongly pressure-dependent.

Results for the fully substituted alkenes (TME and 3,4-dimethyl-3-hexene) are consistent with our measured yields.[1] The exception is at the higher pressures, at which the TME data "level off" in a way that is inconsistent with collisional stabilization. Also, our measurement of extremely small H yields (<1%) is consistent with the hydroperoxide channel being the dominant reaction mechanism. Calculations suggest that the differences in OH yield of the two alkenes is only significant at high pressures (300 Torr) where our data are practically nonexistent.

For the reaction of ozone with ethene, however, theoretical results (from this study and from that of Olzmann et al.[21]) predict yields far lower than observed. Therefore the OH is likely formed by a channel not included in the reaction mechanism modeled by our calculations.

As mentioned in the Mechanism section, one possible additional OH source is the "hot acid" channel (R3a−d), in which isomerization to dioxirane can form OH via a formic acid intermediate. Our calculations suggest that for ethene, formation of dioxirane occurs with high yield and is largely pressure independent. In one quantum chemistry study,[19] it was shown that this barrier is by far the highest in the "hot acid" channel; thus, further steps are expected to be pressure-independent as well. Since formic acid has numerous decomposition channels, only a fraction of the dioxirane formed will decompose to OH. Therefore this channel of OH formation is consistent with our observations of small, pressure-independent OH yields for the ozonolysis of ethene. In addition, measured ozone−ethene products are consistent with the formation of vibrationally excited formic acid (see, for example, ref 34), as are our direct observation of hydrogen atoms.[1]

Recently Fenske et al.[12] determined OH yields from the ozone-ethene reaction to be pressure-dependent, with significantly higher yields at pressures below 100 Torr. In that study the second alternate pathway, the nonconcerted decomposition of the ozonide (reaction R7), was invoked, and the pressure-dependence was attributed to collisional stabilization of the excited hydroperoxide intermediate. However, this intermediate has 50 kcal/mol of energy in excess of the "loose" barrier to OH formation. Thus it is expected to dissociate very quickly, faster than its collisional lifetime; indeed, in ref 21 it was shown that for the dissociation of a similar molecule (the ozonide), no pressure dependence is expected, even when vibrational excitation is lower and the transition state tighter. Thus, neither potential OH-forming channel (decomposition of the "hot acid" or of the ozonide) can account for a pressure dependence; our data do not entirely preclude the possibility of a pressure

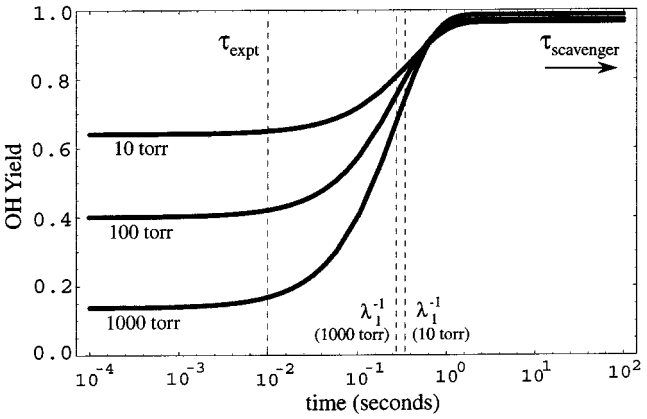

Figure 9. Calculated time-dependent OH yields from TME at 10, 100, and 1000 Torr. Experimental time scales and lifetimes (λ_1^{-1}) versus thermal dissociation to OH are also shown. Note that the experimental time scale in our prompt study (10 ms)[1] is significantly below such lifetimes; for scavenger studies, however, the experimental time scale may exceed such lifetimes by many orders of magnitude.

dependence as well. Given this ambiguity in the data, and the similarity of products expected for both channels, it is difficult to speculate on the nature of this additional OH source.

For the disubstituted alkenes (*trans*-2-butene, *trans*-3-hexene, and *trans*-4-octene), predicted OH yield is somewhat lower than measured yield. This may be a result of uncertainties in absolute measured yield and/or in master equation parameters, most notably the branching ratio between syn and anti carbonyl oxide formation. Still, the anti carbonyl oxides formed from these alkenes may also proceed by the "hot acid" channel, in which the dioxirane (formed in high yield from the anti carbonyl oxide) isomerizes to an excited organic acid. This acid will have fewer possible dissociation channels than formic acid, as alkyl transfers are unlikely; for example, the H_2O + CO pathway is available to excited HCOOH but the corresponding ROH + CO channel may not be available to RCOOH. Thus, dissociation of the excited acid to OH may be more likely in the substituted case. Yield measurements on selectively deuterated alkenes would be particularly instructive in this case.

Time-Dependent OH Yields

While the above calculations support our experimental results, in that prompt OH formation is pressure-dependent, we must ask why scavenger studies measure high, pressure-independent yields. A major difference between our direct study and previous scavenger experiments is the time scale over which measurements are made. In our study measurements are made after reaction times on the order of 10 ms; a typical scavenger study lasts several minutes or longer. This difference may have a profound influence on the amount of OH produced in the reaction: Figure 9 shows OH yield as a function of time for TME + ozone, at 10, 100, and 1000 Torr, using the time-dependent master equation (regimes II−IV) and assuming negligible interference from secondary reactions. Our direct experiments are made within regime II, in which OH is formed from the vibrationally excited carbonyl oxide only. Measurements in scavenger studies, on the other hand, are made deep into regime IV, in which thermalized carbonyl oxide has reached a steady state, and a significant fraction of the OH formed may be from thermal dissociation.

Therefore it is actually not surprising that the scavenger experiments measure higher OH yields. More importantly, the difference in the pressure dependences observed in our laboratory and in scavenger studies[12] is expected: the yield at long steady state is controlled mainly by barrier heights and is independent of pressure, whereas the yield during the pseudo steady state may be strongly pressure dependent.

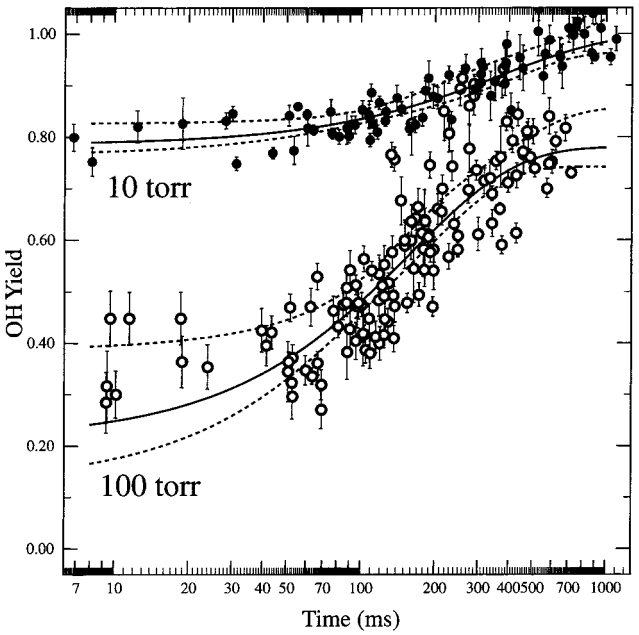

Figure 10. Measured OH yield from ozone + TME as a function of reaction time at 10 Torr (filled circles) and 100 Torr (open circles). Three-parameter fits of the form of eq 5 are shown, with uncertainties.

This prediction is easy to test. We have measured OH yields from the TME + ozone reaction as a function of time, using the same technique presented earlier for measurement of prompt OH yields[1]. Our high-pressure flow (HPF) system is ideal for measuring the time dependence of yields due to its excellent time resolution (on the order of ~1 ms) and well-defined t = 0. While in our companion study reaction times were kept extremely short (~10 ms), reaction times may be increased by reducing the flow velocity and/or increasing the distance between reaction initiation and OH detection. Flow velocity, which remains nearly constant along the tube, is monitored using a pitot-static tube located at the end of the flow.

The only major change to the system here is the addition of three more LIF detection axes. The laser beam passes through the system at four different points within a 70 cm section of the tube, and OH fluorescence is monitored at each point. This allows for the measurement of [OH] at four reaction times simultaneously; this is also useful for OH kinetics and will be described in more detail in future work. In addition, we have improved our LIF calibration substantially, from cross-calibration with the Harvard ER-2 HO_x instrument.[35] This improvement, which will also be described in future work, allows for the measurement of absolute yields.

Results, for time-dependent OH yields from ozone + TME at 10 and 100 Torr, are shown in Figure 10. Fits shown are of the form of eq 5, and fit parameters, along with theoretical predictions, are presented in Table 1. For most reaction times shown, different combinations of reaction distance and flow velocity were used, to minimize the effects of any systematic errors that may arise from one particular flow condition or LIF detection axis. Alkene concentrations are kept low enough such that during the course of the reaction, significant depletion of ozone does not occur, even at the longest reaction times. At very short reaction distances we are unable to obtain high-quality data by slowing the flow. The reason for this is not clear, but

TABLE 1: Values for Y_{II}, Y_{IV}, and λ_1 from Equation 5, Determined for Ozone + TME from Fitting Experimental Data (Theoretical Values Shown for Comparison)

	experiment		theory	
parameter	10 Torr	100 Torr	10 Torr	100 Torr
λ_1 (rate) (s^{-1})	2.7 ± 0.7	6.4 ± 0.9	2.6	3.5
Y_{II} (prompt yield)	0.79 ± 0.01	0.21 ± 0.04	0.65	0.40
Y_{IV} (thermal yield)	0.21 ± 0.02	0.57 ± 0.04	0.32	0.57
$Y_{II} + Y_{IV}$	1.00 ± 0.03	0.78 ± 0.08	0.97	0.97

this may explain the apparent "leveling off" of our measured yields for TME at high pressures,[1] as high pressures are only achieved in our system by slowing the flow. Still, for both pressures shown, the expected increase in OH yield with time is observed, with the increase being far greater at 100 Torr.

Discussion

Our theoretical and experimental results show that the time-dependent master equation must be used in order to model the formation of OH from carbonyl oxides even qualitatively. In our experiment, OH production clearly increases on longer time scales, and the observed time and pressure dependences are consistent with theoretical predictions, providing strong evidence that thermal decomposition of stabilized carbonyl oxides is taking place. Much of the OH measured in environmental chambers likely comes from decomposition of stabilized carbonyl oxides also, reconciling our measured yields with those measured in scavenger studies.

The possibility of OH formation from thermalized carbonyl oxide has been recognized before: Olzmann et al.[21] calculate that on the time scales of most scavenger experiments, thermal formation of OH may occur. However, they discount this possibility, instead assuming that all carbonyl oxide will be removed via bimolecular reaction before dissociation is possible. Part of the reason for this assumption is presumably that their results reasonably matched the available experimental evidence. However, this agreement is poor, considering scavenger studies determine OH yields from TME to be higher than their predictions (66%−78%) and independent of pressure. They also argue that the high CO and CO_2 yields observed in ozone + TME product studies[36] suggest reactions of the carbonyl oxide, as calculated dioxirane yields are small. However, this assumes that of the unimolecular channels, only dioxirane produces CO and CO_2; this is probably not the case, as the OH-forming channel produces $RCOCH_2$ radicals, which have been shown to form CO and CO_2 upon further reaction.[7]

To our knowledge our time-dependent measurements constitute the first direct observations of the expected time dependence of product yield (in regimes II through IV) for a chemical activation reaction. Values of the fit parameters (presented in Table 1) may be interpreted physically: most important is the value for λ_1, which corresponds to the rate constant for dissociation of the thermalized carbonyl oxide to form OH. Our measured values are in close agreement with our calculations, though are significantly smaller than the theoretical estimate of Olzmann et al.[21] ($250\ s^{-1}$); this theoretical value, however, is extremely sensitive to the value of the barrier height to dissociation, and even a 2 kcal/mol error could account for such a difference. As predicted by theory, λ_1 is found to be pressure-dependent, indicating that at 100 Torr the dissociation reaction has not reached the high-pressure limit. The difference between λ_1's at 10 and 100 Torr is found to be greater than that predicted by theory; at this point it is difficult to speculate whether that is a result of uncertainty in the data or in the master equation parameters.

To date there exists only one other measurement of the rate of thermal unimolecular reaction of a carbonyl oxide. Fenske et al.,[37] by measuring the concentration of the secondary ozonide (which is formed by the reaction of carbonyl oxide with an aldehyde) in *trans*-2-butene ozonolysis at 1 atm, have determined the rate of unimolecular reaction to be $76\ s^{-1}$, accurate to within a factor of 3. It is difficult to compare the rate measured in that study and our result: while the carbonyl oxide from *trans*-2-butene, with fewer vibrational modes, is expected to react more slowly than that from TME, the higher pressure in that study may offset this difference somewhat. Furthermore, our study shows that the thermal carbonyl oxide dissociates to form OH; when determining the unimolecular rate constant, Fenske et al. do not consider this possibility in their chemical model, which may have an effect on their calculated rate. Still, the rough agreement in measured time scales for decomposition (tens to hundreds of milliseconds) in these two studies is encouraging.

One major discrepancy between our theoretical predictions and our experimental results is the OH yield at 100 Torr at long times (true steady state). We predict that yield should grow to nearly unity but measure it at ~0.80. There are three possible explanations for this behavior. First, we have not yet obtained data beyond 800 ms at 100 Torr; from the existing data it is difficult to tell if the thermalized carbonyl oxide has yet reached steady state, and so the fit may be off. Second, the pressure-dependent LIF calibration may be slightly inaccurate, leading to small (~20%) underestimates at 100 Torr. This error would in fact affect our prompt yield measurements at high pressures,[1] but only slightly. A third possibility is that the measured pressure dependence in long-time yield is real. Indeed, in two scavenger studies[3,4] the OH yield for ozone + TME is measured to be 80−90%. A pressure dependence in the long-time yield may arise if there exists another pathway by which the intermediate can proceed, which is lower in energy but entropically much "tighter." This pathway would be minor for the chemically activated species but more important for the thermal species, reducing the thermal yield at higher pressures. However, there exists no evidence of such an additional pathway; calculations in this study as well as in Olzmann et al.[21] indicate that the ring-closure to dioxirane is higher in energy than dissociation to OH. Moreover, in one scavenger study[12] it was found that OH yield is nearly unity at both 20 Torr and 760 Torr. Further time-dependent yield studies are certainly necessary and are currently underway.

Distinguishing between OH formed promptly (by vibrationally excited carbonyl oxide) or slowly (by thermal carbonyl oxide) aids in the interpretation of other experimental results. For example, the long steady state yield arises from a thermal distribution of carbonyl oxide, in which the vibrational energy does not vary from reaction to reaction. Thus, in the long steady state, only the structure of the carbonyl oxide determines yield. Hence, SAR's (such as in ref 4), which neglect energetics and alkene size and predict OH yields solely on available reaction pathways, are expected to hold. This is particularly true when the majority of the OH produced is from thermal reaction, which from our measurements of prompt yields seems to be the case for larger alkenes.

In addition, this separation of time scales has implications for indirect measurements of stabilized carbonyl oxide yields. The most extensive measurements use SO_2 as the carbonyl oxide scavenger, with yields determined by production of H_2SO_4[20]

or of carbonyl,[4] both products of the $CR_2OO + SO_2$ reaction. Studies are carried out using a large excess of SO_2, such that the thermalized carbonyl oxide likely reacts befor reaching steady state; i.e., the yield is measured in regime II or III. This is consistent with the pressure dependence of the carbonyl oxide yield measured by Hatakeyama et al.[20] for *trans*-2-butene. Thus it is difficult to draw conclusions from comparisons of OH yields measured in scavenger studies (long steady state) and measured carbonyl oxide yields (pseudo steady state).[4,6,7]

To assess which time scale is appropriate for describing OH formation in the earth's atmosphere, we must consider the effects of bimolecular reactions of the thermalized carbonyl oxide. If the carbonyl oxide is reacted away faster than it can thermally dissociate, only the OH produced during the pseudo steady state (regime II) will be significant in the troposphere. If instead the bimolecular reactions of the carbonyl oxide are slow relative to thermal dissociation, the OH formed in regime IV will also be atmospherically important. Recent experimental evidence suggests that the latter is the case; Johnson et al.[38] have found that for 2-methyl-2-butene, measured OH yield does not change even in the presence of an excess (20,000 ppm) of water or high concentrations (100−500 ppm) of SO_2, butanone, or acetic acid. Neeb and Moortgat[7] also report the same result when water is added to their experiment. Indeed, in our own time-dependent OH yield measurements, leaks invariably led to some water being present in our flow tube. For a given reaction time shown, different flow rates were used, leading to varying water concentrations, yet OH yield did not change. These results are significant in that water is the most abundant atmospheric species believed to react with carbonyl oxides. In addition, these results suggest that no OH is formed from the reaction of water with carbonyl oxide (or other intermediates of ozonolysis), as has been suggested in the past.[39] Therefore, the measured differences in prompt and thermal OH yields are almost certainly from thermal decomposition of the carbonyl oxide and not from secondary bimolecular reactions. Thus, experimental evidence suggests that in the troposphere, thermalized carbonyl oxide will in fact dissociate to OH.

Conclusions

We have presented RRKM/master equation calculations which describe OH generation from the ozone-alkene reaction, on both short and long time scales. For all substituted alkenes, significant prompt yields of OH are expected. These yields are highly pressure-dependent, and thus also dependent on substituent size; this is consistent with our experimental results. In the case of ethene, whose carbonyl oxide (CH_2OO) has a much higher barrier to OH formation than substituted alkenes, the accepted reaction mechanism leads to yields far lower than observations. This suggests an additional pathway of OH formation, which may also play somewhat of a role in OH formation from disubstituted alkenes.

Our model also suggests the cause for the stark discrepancy between the direct measurements and the results obtained in the scavenger studies. Time-dependent master equation calculations show that scavenger studies are sufficiently long that the stabilized carbonyl oxide may undergo thermal dissociation, leading to high, pressure-independent OH yields. Our prediction that OH yields should be time-dependent is fully borne out by experiment: we find that yields increase with time in a manner consistent with theory, and this increase is far more significant at higher pressure. We measure the rate constant for unimolecular decomposition of the carbonyl oxide to be 2.7 s^{-1} at 10 Torr and 6.4 s^{-1} at 100 Torr, in reasonably good agreement with theory as well as previous experimental results.

The dependence of OH yields on experimental time scale aids in the interpretation of experimental results and resolves apparent contradictions in measured pressure dependences of ozonolysis products. Experimental evidence suggests that in the atmosphere, OH production from thermalized carbonyl oxide is significant, and the yields measured in scavenger studies (and, in the future, in our direct, time-dependent measurements) are the appropriate ones to use for tropospheric modeling. However, other bimolecular channels must now always be considered. In the atmosphere, reaction with relatively abundant gases such as water vapor must be carefully assessed, while in scavenger experiments secondary removal by a number of reactions could play a role.

To better assess how much of the OH measured in scavenger studies is from either mechanism of OH formation, it is necessary to measure more pressure- and time-dependent yields, for a wider variety of alkenes than those we have studied already. Branched alkenes, cycloalkenes, asymmetric alkenes, and terpenes are all more complicated, due to more reaction pathways and/or more complicated energetics.

Finally, the mechanism of OH formation by the reaction of ozone with ethene (and terminal alkenes) remains poorly understood. The dissociation of formic acid and the nonconcerted decomposition of the ozonide have both been put forth as possible candidates, and the evidence does not clearly favor one over the other. In fact, the differences in measured pressure dependence in this study and in that of Fenske et al.[12] cannot be accounted for by either channel. Understanding this mechanism is important because CH_2OO is formed in the ozonolysis of terminal alkenes, which include tropospherically abundant species such as isoprene. Additional studies (both theoretical and experimental) of the gas-phase ozone−ethene reaction, the most basic of the ozone-alkene reactions, are certainly necessary.

Acknowledgment. The authors are grateful to T. F. Hanisco for experimental assistance. This work was supported by U.S. EPA STAR Grant R825258010 (University at Albany-SUNY and Harvard University), as well as NSF Grant 9977992 (Harvard University). J.H.K. gratefully acknowledges support from the NASA Earth System Science Fellowship Program.

Appendix A: Solution to the Time-Dependent Master Equation

In this section we present a short derivation of eq 2, the solution to the time-dependent master equation. We begin with eq 1:

$$\frac{d\mathbf{N}(t)}{dt} = R\mathbf{F} - \mathbf{J}\mathbf{N}(t) \tag{6}$$

Terms are as defined in the Theoretical section. The solution to a differential equation of this type is standard:

$$\mathbf{N}(t) = e^{-\mathbf{J}t}\mathbf{N}(0) + \{e^{-\mathbf{J}t}\int_0^t e^{\mathbf{J}s}R(s)ds\}\mathbf{F} \tag{7}$$

By assuming that the initial concentration of the intermediate is zero and that the rate of formation of the intermediate (R) is constant, we obtain the result found in ref 27:

$$\mathbf{N}(t) = R\{\mathbf{I} - e^{-\mathbf{J}t}\}\mathbf{J}^{-1}\mathbf{F} \tag{8}$$

As with the time-dependent master equation describing simple unimolecular dissociation,[40] this solution may be expressed in terms of the right eigenvector matrix ($\mathbf{U}$) and diagonal eigen-

value matrix (Λ) of **J**, from the identity $\mathbf{JU} = \mathbf{U}\Lambda$:

$$\mathbf{N}(t) = R\{\mathbf{I} - \mathbf{U}e^{-\Lambda t}\mathbf{U}^{-1}\}\mathbf{U}\Lambda^{-1}\mathbf{U}^{-1}\mathbf{F} \quad (9)$$

$$= R\mathbf{U}\{\mathbf{I} - e^{-\Lambda t}\}\Lambda^{-1}\mathbf{U}^{-1}\mathbf{F} \quad (10)$$

Since **I**, $e^{-\Lambda t}$, and Λ^{-1} are all diagonal matrixes, eq 10 may be rewritten in terms of λ, the diagonal elements of Λ:

$$\mathbf{N}(t) = R\mathbf{U}\mathrm{diag}\left\{\frac{1 - e^{-\lambda t}}{\lambda}\right\}\mathbf{U}^{-1}\mathbf{F} \equiv R\mathbf{U}\mathbf{L}\mathbf{U}^{-1}\mathbf{F} \quad (11)$$

This is the expression given in eq 2. Note that, at long times ($t \rightarrow \infty$), $\mathbf{L} = \Lambda^{-1}$, and eq 11 simplifies to the steady-state expression, $\mathbf{N} = R\mathbf{J}^{-1}\mathbf{F}$.

Appendix B: Determination of Master Equation Parameters

Microcanonical reaction rates are determined using standard RRKM theory. Rovibrational sums and densities of states are calculated using standard counting techniques (the BS−SR algorithm[41]), with internal rotations and one active external rotation treated as free classical rotors. Geometries, frequencies, and rotational constants are calculated using the B3LYP/6-31G(d) model chemistry, and single-point energies using B3LYP/6-311G+(3df,2p). Calculated frequencies and zero-point energies are scaled by the recommended 0.9613 and 0.9804, respectively.[42]

Optimized, zero-point-corrected energies are presented in Table 2. These numbers generally agree with other published values to within a few kcal/mol; the effects of such uncertainties on our calculations are considered in Appendix C. Pathways for both the syn and the anti conformers of the *trans*-2-butene carbonyl oxide are shown; these are assumed not to interconvert.[33] We also perform calculations on the carbonyl oxides formed from *trans*-3-hexene, *trans*-4-octene, and 3,4-dimethyl-3-hexene. However, in these cases we do not calculate energies explicitly but instead use those of *trans*-2-butene (for *trans*-3-hexene and *trans*-4-octene) and TME (for 3,4-dimethyl-3-hexene), which should be similar. We also neglect the possibility of an OH-formation channel via a 6- (or 7-) membered transition state, as these should have only a minor effect on yields. Instead, we treat these alkenes exactly like *trans*-2-butene or TME, only with more internal modes and smaller rotational constants characteristic of extra methylene groups.

The model used to describe energy transfer probability, **P**, is the "exponential down" model,[40] in which the probability of a downward change in energy decays exponentially with the change in energy, and is scaled by $\langle\Delta E\rangle_d$, the average energy change per deactivating collision with the bath gas. Upward transitions are possible also, and are determined by detailed balance. We use the hard-sphere collision frequency for the collision frequency ω.

The nascent energy distribution of the carbonyl oxide is determined by two factors: the energy distribution of the parent ozonide and the partitioning of this energy between the carbonyl oxide and carbonyl fragments. Assuming statistical partitioning of energy, the latter factor (distribution of energy in the internal modes of the nascent carbonyl oxide, or g_{dist}) may be expressed as:[43]

$$g_{dist}(E, E_T) = \frac{\rho_1(E)W_2(E_T - E)}{\int_0^{E_T} dE'\rho_1(E')W_2(E_T - E')} \quad (12)$$

TABLE 2: Energies Used in Master Equation Calculations[a]

molecule	ethene	t2b (anti)	t2b (syn)	TME
TS_a (OH)	34.0	22.5	16.7	16.0
TS_b (dioxirane)	20.7	16.9	24.7	21.7
E_{avail}	39.1	39.5	38.9	42.8

[a] All energies in kcal/mol and are relative to the carbonyl oxide.

in which E_T is the total energy available to the system, ρ is the density of states, and W the sum of states, with subscript 1 referring to the carbonyl oxide and 2 the carbonyl.

However, partitioning is probably not statistical: the steepness of the repulsive surface beyond a tight transition state prevents complete randomization of energy among all the modes; fragments tend to be vibrationally "colder" than statistical theory would predict, with higher relative translational motion than expected.[43,44] Rather than apply a sophisticated model of nonstatistical energy partitioning (such as in ref 45), we assume that only the energy in excess of the barrier is partitioned statistically and the rest goes into product translation. This approach is a reasonable one, since in general, a majority of the energy (~60%[45]) released going from the TS to products is in the form of relative translation. This approach is also supported by our yield measurements,[1] in which yields seem largely insensitive to carbonyl oxide stability. Still, this assumption may underestimate the total energy available to the carbonyl oxide, as ~20% of the energy liberated beyond the TS should go to internal modes of the carbonyl oxide; we address this point of uncertainty in Appendix C.

The overall energy distribution of nascent carbonyl oxide, $F(E)$, may be obtained by combining g_{dist} from eq 12 with g_{oz}, the normalized energy distribution of the parent ozonide:

$$F(E) = \int_{E_0}^{\infty} dE' g_{oz}(E') g_{dist}(E, E') \quad (13)$$

in which E_0 is the barrier to ozonide fragmentation. Because g_{dist} is much broader than g_{oz}, $F(E)$ is insensitive to the shape (though not the average energy) of g_{oz}. OH yields using the above energy distribution agree very closely (within a few percent) with those calculated by simply approximating g_{oz} as a delta function, centered on the average energy of the exact distribution. Furthermore, as discussed in the Theoretical section, collisional stabilization of the ozonide is negligible, so g_{oz} in eq 13 may be approximated by the nascent ozonide energy distribution.

Thus we approximate the energy distribution of the ozonide as a delta function, centered on the average energy of the reacting ozone + alkene system, and do not perform any statistical calculations for the ozonide. Note that eq 13 is still sensitive to the value of this average energy, so density-functional calculations of ozone, the alkene, and the ozonide decomposition TS are also necessary. Energy available for each carbonyl oxide is also included in Table 2; values for TME and ethene agree (to within a few kcal/mol) with those in ref 21. For *trans*-2-butene we calculate that the syn conformer is formed with slightly less energy than the anti conformer, because of a small difference in calculated barrier heights to ozone formation. It should be noted that this result is the reverse that obtained in two other studies on the same system,[46,47] though differences are small. RRKM calculations on the ozonide predict that 59% of the ozonide will dissociate to form the anti product.

Appendix C: Sensitivity of Results to Master Equation Parameters

Here we present results from sample master equation calculations on TME + ozone, in which we test the sensitivity of

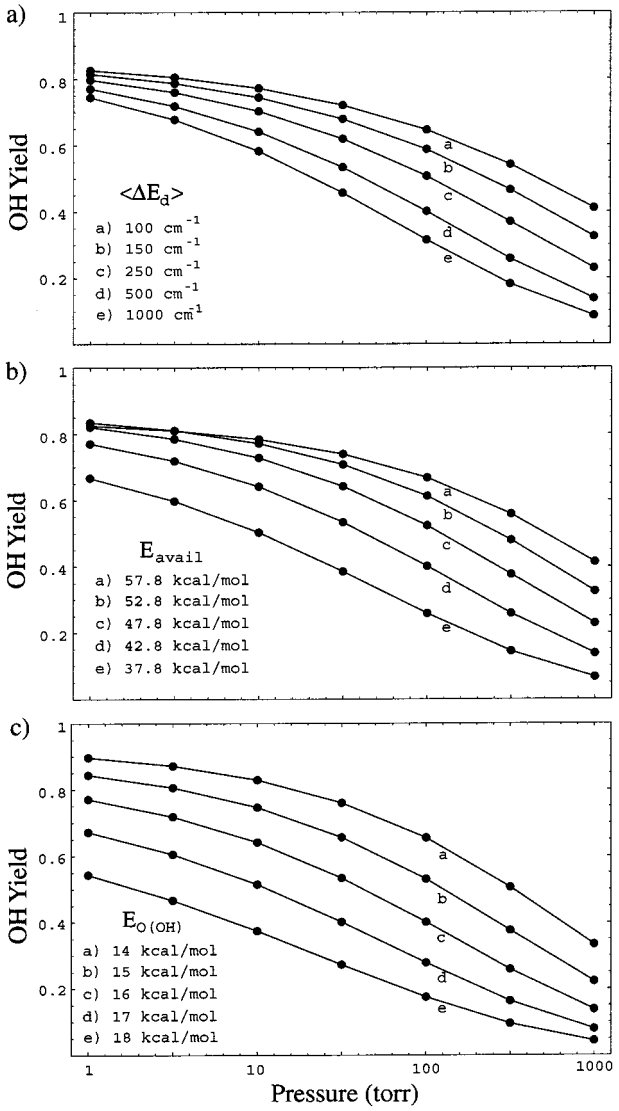

Figure 11. Sensitivity of calculated pressure-dependent OH yields to (a) $\langle\Delta E\rangle$ (average energy change per deactivating collision), (b) E_{avail} (energy available the internal modes of ozonide decomposition fragments), and (c) $E_{0(OH)}$ (barrier height of OH formation channel). All calculations were performed for TME + ozone.

calculated yields to various uncertain parameters. The three values with the most uncertainty are $\langle\Delta E\rangle_d$ (the average energy lost from deactivating collision with a bath gas molecule), E_{avail} (the energy available for partitioning among the internal modes of the ozonide fragments), and $E_{0(OH)}$ (the barrier height of the OH-forming channel). Other potential sources of error certainly exist, but they are expected to have a smaller effect on results.

In Figure 11a we show pressure-dependent OH yields for a number of $\langle\Delta E\rangle_d$'s, in which E_{avail} and $E_{0(OH)}$ are held at their values from electronic structure calculations (42.8 and 16.0 kcal/mol, respectively). The range used (0.26−2.6 kcal/mol) certainly includes the appropriate $\langle\Delta E\rangle_d$ for an N_2−carbonyl oxide collision[21]. While the predicted pressure dependence is influenced by $\langle\Delta E\rangle_d$, a pressure dependence is always predicted. Note that at 1 Torr, yield is practically independent of $\langle\Delta E\rangle_d$, suggesting that the reaction has reached its low-pressure limit, in which few deactivating collisions occur.

Figure 11b shows the dependence of yield to total energy available to partition between the carbonyl oxide and the carbonyl (E_{avail}). Here $\langle\Delta E\rangle_d$ is held at 500 cm^{-1} and $E_{0(OH)}$ at 16.0 kcal/mol. The range in values used is large, as the value of E_{avail} is dependent on a number of parameters: ozone−alkene barrier height, ozonide stability, barrier to ozonide fragmentation, and amount of ozonide vibrational energy which ends up in fragment vibrations. As discussed in Appendix B, this last term is especially uncertain. We assume that only the energy in excess of the barrier to fragmentation is distributed, which yields our calculated E_{avail} of 42.8. At the highest value of E_{avail} shown, an additional 40% of the energy released beyond the TS goes into internal energy. Again, while predicted pressure dependence is affected by available energy, at no reasonable value of E_{avail} is it small. Note that at high energies, low-pressure yields actually decrease with increasing energy; this is due to the increasing importance of the dioxirane channel, which is "looser" than the OH channel and is therefore favored at higher energies.

Finally, Figure 11c shows the effect of varying $E_{0(OH)}$, the barrier height to OH formation. Here $\langle\Delta E\rangle_d$ is fixed at 500 cm^{-1} and E_{avail} at 42.8 kcal/mol. The range is ±2 kcal/mol, a reasonable uncertainty for B3LYP barrier heights. Results are fairly sensitive to barrier height, but again in all cases a strong pressure dependence is predicted. The decrease in the low-pressure yield comes largely from a larger proportion of the carbonyl oxide formed vibrationally "cold." It should be noted that lowering the barrier height is roughly equivalent to including the effects of tunneling, which may be important for this intramolecular H-transfer reaction.

Thus while predicted OH yields are dependent on the parameters $\langle\Delta E\rangle_d$, E_{avail}, and $E_{0(OH)}$, yields are always expected to be pressure-dependent. Similar calculations have been performed for ethene, with the same result: the qualitative results do not change significantly. Thus, barring a combination of extremely large errors, the uncertainties inherent in a number of master equation parameters do not change our overall results, at least in a qualitative sense.

References and Notes

(1) Kroll, J. H.; Clarke, J. S.; Donahue, N. M.; Anderson, J. G.; Demerjian, K. L. *J. Phys. Chem. A* **2001**, *105*, 1554.
(2) Atkinson, R.; Aschmann, S. M. *Environ. Sci. Technol.* **1993**, *27*, 1357.
(3) Chew, A. A.; Atkinson, R. *J. Geophys. Res.* **1996**, *101*, 28649.
(4) Rickard, A. R.; Johnson, D.; McGill, C. D.; Marston, G. *J. Phys. Chem. A* **1999**, *103*, 7656.
(5) Paulson, S. E.; Fenske, J. D.; Sen, A. D.; Callahan, T. W. *J. Phys. Chem. A* **1999**, *103*, 2050.
(6) Paulson, S. E.; Chung, M. Y.; Hassan, A. S. *J. Phys. Chem. A* **1999**, *103*, 8125.
(7) Neeb, P.; Moortgat, G. K. *J. Phys. Chem. A* **1999**, *103*, 9003.
(8) Donahue, N. M.; Kroll, J. H.; Anderson, J. G.; Demerjian, K. L. *Geophys. Res. Lett.* **1998**, *25*, 59.
(9) Mihelcic, D.; Heitlinger, M.; Kley, D.; Musgen, P.; Volz-Thomas, A. *Chem. Phys. Lett.* **1999**, *301*, 559.
(10) Paulson, S. E.; Orlando, J. J. *Geophys. Res. Lett.* **1996**, *23*, 3727.
(11) Ariya, P. A.; Sander, R.; Crutzen, P. J. *J. Geophys. Res.* **2000**, *105*, 17721.
(12) Fenske, J. D.; Hasson, A. S.; Paulson, S. E.; Kuwata, K. T.; Ho, A. W.; Houk, K. N. *J. Phys. Chem. A* **2000**, *104*, 7821.
(13) Criegee, R. *Angew. Chem. Int. Ed.* **1975**, 14: 745.
(14) Martinez, R. I.; Herron, J. T.; Huie, R. E. *J. Am. Chem. Soc.* **1981**, *103*, 3807.
(15) Niki, H.; Maker, P. D.; Savage, C. M.; Breitenbach, L. P.; Hurley, M. D. *J. Phys. Chem.* **1987**, *91*, 941.
(16) Gutbrod, R.; Schindler, R. N.; Kraka, E.; Cremer, D. *Chem. Phys. Lett.* **1996**, *252*, 221.
(17) Martinez, R. I.; Herron, J. T. *J. Phys. Chem.* **1987**, *91*, 946.
(18) Gutbrod, R.; Schindler, R. N.; Kraka, E.; Cremer, D. *J. Am. Chem. Soc.* **1997**, *119*, 7330.
(19) Cremer, E.; Kraka, E.; Szalay, P. G. *Chem. Phys. Lett.* **1998**, *292*, 97.
(20) Hatakeyama, S.; Kobayashi, H.; Akimoto, H. *J. Phys. Chem.* **1984**, *88*, 4736.

(21) Olzmann, M.; Kraka, E.; Cremer, D.; Gutbrod, R.; Andersson, S. *J. Phys. Chem. A* **1997**, *101*, 9421.
(22) Herron, J. T.; Huie, R. E. *J. Am. Chem. Soc.* **1977**, *99*, 5430.
(23) O'Neal, H. E.; Blumstein, C. *Int. J. Chem. Kinet.* **1973**, *5*, 397.
(24) Harding, L. B.; Goddard, W. A. III. *J. Am. Chem. Soc.* **1978**, *100*, 7180.
(25) Anglada, J. M.; Crehuet, R.; Bonfill, J. M. *Chem. Eur. J.* **1999**, *5*, 1809.
(26) Hoare, M. *J. Chem. Phys.* **1963**, *38*, 1630.
(27) Serauskas, R. V.; Schlag, E. W. *J. Chem. Phys.* **1965**, *42*, 3009.
(28) Schranz, H. W.; Nordholm, S. *Chem. Phys.* **1984**, *87*, 163.
(29) Snider, N. *J. Chem. Phys.* **1984**, *80*, 1885.
(30) Troe, J. *J. Chem. Phys.* **1977**, *66*, 4745.
(31) Fulle, D.; Hamann, H. F.; Hippler, H.; Troe, J. *J. Chem. Phys.* **1996**, *105*, 983.
(32) Orlando, J. J.; Tyndall, G. S.; Vereecken, L.; Peeters, J. *J. Phys. Chem. A* **2000**, *104*, 11578.
(33) Anglada, J. M.; Bonfill, J. M.; Olivella, S.; Sole, A. *J. Am. Chem. Soc.* **1996**, *118*, 4636.
(34) Neeb, P.; Horie, O.; Moortgat, G. K. *J. Phys. Chem. A* **1998**, *102*, 6778.
(35) Wennberg, P.; Cohen, R. C.; Hazen, N. L.; Lapson, L. B.; Allen, N. T.; Hanisco, T. F.; Oliver, J. F.; Lanham, N. W.; Demusz, J. N.; Anderson, J. G.. *Rev. Sci. Instr.* **1994**, *65*, 1858.
(36) Gutbrod, R.; Meyer, S.; Rahman, M. M.; Schindler, R. N. *Int. J. Chem. Kinet.* **1997**, *29*, 717.
(37) Fenske, J. D.; Hasson, A. S.; Ho, A. W.; Paulson, S. E.. *J. Phys. Chem. A* **2000**, *104*, 9921.
(38) Johnson, D.; Lewin, A. G.; Marston, G. *J. Phys. Chem. A* **2001**, *105*, 2933.
(39) Paulson, S. E.; Flagan, R. C.; Seinfeld, J. H. *Int. J. Chem. Kinet.* **1992**, *23*, 103.
(40) Holbrook, K. A.; Pilling, M. J.; Robertson, S. H. *Unimolecular Reactions*; John Wiley & Sons: Chichester, 1996.
(41) Stein, S. E.; Rabinovitch, B. S. *J. Chem. Phys.* **1973**, 58: 2438.
(42) Wong, M. W. *Chem. Phys. Lett.* **1996**, 256: 391.
(43) Forst, W. *Theory of Unimolecular Reactions*; Academic Press: New York, 1973.
(44) Baer, T.; Hase, W. L. *Unimolecular Reaction Dymanics: Theory and Experiments*; Oxford University Press: New York, 1996.
(45) Mordaunt, D. H.; Osborn, D. L.; Neumark, D. M. *J. Chem. Phys.* **1998**, *108*, 2448.
(46) Rathman, W. C. D.; Claxton, T. A.; Rickard, A. R.; Marston, G. *Chem. Phys. Phys. Chem.* **1999**, *1*, 3981.
(47) Fenske, J. D.; Kuwata, K. T.; Houk, K. N.; Paulson, S. E. *J. Phys. Chem. A* **2000**, *104*, 7246.